


# VCSEL quick fabrication of 894.6 nm wavelength epi-material for miniature atomic clock applications

Jack Baker<sup>1</sup>  | Craig P. Allford<sup>1</sup> | Sara Gillgrass<sup>1</sup> | Tomas Peach<sup>2</sup> |  
James Meiklejohn<sup>1</sup> | Curtis Hentschel<sup>1</sup> | Wyn Meredith<sup>3</sup> | Denise Powell<sup>3</sup> |  
Tracy Sweet<sup>4</sup> | Mohsin Haji<sup>5</sup> | J. Iwan Davies<sup>4</sup> | Samuel Shutts<sup>1</sup> | Peter M. Snowton<sup>1,2</sup>

<sup>1</sup>Future Compound Semiconductor Manufacturing Hub, Cardiff University, Cardiff, UK

<sup>2</sup>Institute for Compound Semiconductors, Cardiff University, Cardiff, UK

<sup>3</sup>Compound Semiconductor Centre, Pascal Close, Cardiff, UK

<sup>4</sup>IQE plc, Pascal Close, Cardiff, UK

<sup>5</sup>National Physical Laboratory, Teddington, UK

## Correspondence

Jack Baker, School of Physics and Astronomy,  
Cardiff University, Queen's Buildings, The Parade,  
Cardiff CF24 3AA, UK.  
Email: [bakerj19@cardiff.ac.uk](mailto:bakerj19@cardiff.ac.uk)

## Funding information

European Regional Development Fund, Grant/  
Award Number: 82371; Engineering and Physical  
Sciences Research Council, Grant/Award Numbers:  
EP/P006973/1, EP/S513611/1, EP/T517525/1;  
Strength in Places Fund, Grant/Award Number:  
107134

## Abstract

A vertical cavity surface emitting laser (VCSEL) quick fabrication (VQF) process is applied to epitaxial materials designed for miniature atomic clock applications (MACs). The process is used to assess material quality and uniformity of a full 100 mm (4-inch) wafer against the stringent target specification of VCSELs for MACs. Target specifications in optical power ( $>0.6$  mW) and differential efficiencies ( $<0.5$  W/A) are achieved over large portions of a wafer; however, the variation in the oxide aperture diameter is shown to limit the yield. The emission of the fundamental mode at 894.6 nm at 70 °C is met over a significant area of the wafer for  $\sim 4$   $\mu$  m aperture multi-mode devices. The consideration of the on-wafer variation reveals that further optimisation is required to increase the device yield to levels required for volume manufacture.

## 1 | INTRODUCTION

Over 4 decades, the performance of vertical cavity surface emitting lasers (VCSELs) has been refined and commercialised, and the widespread use in data transfer and 3D sensing applications has driven an expansion of the market in recent years. Additionally, modulated VCSELs have also been shown to be ideal light sources for quantum sensing applications in the production of miniature atomic clocks (MACs) due to their low power consumption and circular beam shape [1, 2]. These MACs utilise coherent population trapping (CPT) of the  $D_1$  or  $D_2$  lines in Cs or Rb vapour cells [3] with VCSELs as the optical source of excitation [4]. Although there have been efforts to produce VCSELs emitting on the Cs  $D_1$  line, at 894.6 nm, there still remains a gap in the market. As part of DARPA CSACs projects, Sandia National Laboratories developed high-performance 894.6 nm VCSELs [2]; however, these were not made

commercially available. Additionally, there was a detailed reporting from Ulm University on the design and characterisation novel custom-made single-mode polarisation-stable 894.6 nm VCSELs for MAC applications [5, 6]. As recently as 2019, new capability in producing VCSELs for CPT-based MACs was reported by the National Physical Laboratory in the UK, which sought to address the commercial scarcity; however, further iterations of the epitaxial structure were required to minimise device internal loss, reduce linewidth, and increase the single-mode yield [7]. This need for refinement in the design of the epitaxial structure, which is required for the simultaneous precise control of both spectral characteristics and device efficiency, necessitates improved monitoring in the manufacturing process. One of the most useful methods for this is the characterisation of actual working VCSEL devices; however, this is a time-consuming process, which is incompatible with a commercial setting. To address this issue, a VCSEL Quick

This is an open access article under the terms of the Creative Commons Attribution License, which permits use, distribution and reproduction in any medium, provided the original work is properly cited.

© 2022 The Authors. *IET Optoelectronics* published by John Wiley & Sons Ltd on behalf of The Institution of Engineering and Technology.

Fabrication process (VQF) was previously designed [8] such that, for a given epitaxial structure, key characteristics of device performance can be rapidly assessed and used as feedback for growth conditions. The VQF process was previously demonstrated for 940 nm high-power applications [8, 9], and here, we show its efficacy for the more stringent test in the production of  $\sim 895$  nm emitting VCSEL epi for MACs.

With VCSEL quick fabrication on epi-structures designed for very specific operating conditions like MACs, the design of the VQF device need not resemble that of the final device in the intended application. Rather, VQF aims to result in device performance which assesses epitaxial material quality against the target specifications, for example the very specific operating wavelength. Hence, the performance of a VQF device will not be identical to that of a standard fabrication device, but will provide insight into the quality of the epi in a rapid way, such that refinements can be made with a minimal impact on manufacturing efficiency. The VQF design reduces the processing time by  $\sim 60\%$  relative to a standard dielectric-planarised VCSEL process at the price of limited RF modulation bandwidth, due to the electrical parasitics and non-representative linewidth and mode profile/beam shape. Often a surface relief [5, 10] is utilised in standard MAC devices to achieve the polarisation-stable single-mode emission; however, in the case of VQF devices, the transverse mode profile is determined solely by the oxide aperture.

However, the characteristics that are of concern and those which can provide insight into material quality and indicate that key device specifications are met are the lasing wavelength, threshold current (density), output powers, device efficiencies, and their variations with temperature.

## 2 | EPITAXIAL STRUCTURE

The epitaxial structure was MOCVD-grown, with a generic p-i-n layout, designed for 894.6 nm emission wavelength. This consisted of a 3-QW InGaAs active region sandwiched between an upper carbon-doped  $\text{Al}_{0.12}\text{Ga}_{0.88}\text{As}/\text{Al}_{0.9}\text{Ga}_{0.1}\text{As}$  DBR mirror and lower Silicon-doped  $\text{Al}_{0.12}\text{Ga}_{0.88}\text{As}/\text{Al}_{0.9}\text{Ga}_{0.1}\text{As}$  DBR mirror, grown on an n-type GaAs substrate. The DBR layers are designed for  $\lambda/4$  thickness. A  $\lambda$ -thick inner cavity is formed between the DBR mirrors, consisting of the MQW layers and AlGaAs separate confinement heterostructure layers. A buried  $\text{Al}_{0.98}\text{Ga}_{0.02}\text{As}$  layer is included between the active region and the upper DBR mirror stack positioned at an antinode of the electric field, which is used to provide current confinement and optical guiding, following partial wet thermal oxidation. A schematic of the key features of the VCSEL epitaxial structure is shown in Figure 1.

## 3 | DEVICE FABRICATION

For the qualification of the VQF process against standard VCSEL performance, both types of the structure are processed for this study. The ‘standard’ device structure employs typical

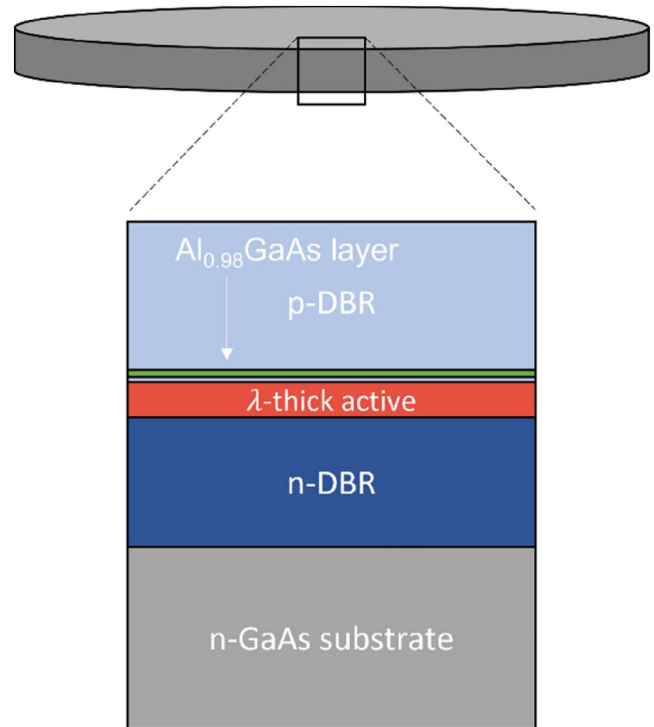


**FIGURE 1** Epitaxial structure of devices produced in this study

processing techniques for dielectric-planarised VCSELs. A p-type ohmic ring contact (Cr/Au) is deposited by physical vapour deposition (PVD), and this is followed by inductively couple plasma (ICP) etching of fully isolated circular mesas, exposing the buried  $\text{Al}_{0.98}\text{Ga}_{0.02}\text{As}$  layer. Wet thermal oxidation of the mesa structures to an oxidation length of  $8.5 (\pm 0.5) \mu\text{m}$  is performed to define the laser aperture. The oxidation length and resulting oxide aperture are monitored in situ with an infrared camera. The mesas are then planarised with a spin coat and a subsequent ICP etch back of benzocyclobutane (BCB). A Ti/Au contact pad and interconnect to the mesa ring contact are then deposited by PVD on the BCB to facilitate electrical probing. An n-Ohmic global contact (AuGe/Ni/Au) is deposited on the back of the GaAs substrate by PVD.

The VQF device process uses similar techniques; however, the device geometry is such that the time-consuming steps of planarisation can be and are omitted, which drastically reduce the total processing time. The device geometry defines the electrical contact, interconnect, and VCSEL mesa regions, and it is patterned by optical lithography. This is then subsequently etched by ICP to expose the buried oxidation layer. Using wet thermal oxidation, with an oxidation length of  $13.5 (\pm 0.5) \mu\text{m}$ , the contact region is fully electrically isolated and only the VCSEL aperture is left unoxidised. This oxidation length is dependent on the geometry of the device and can be reduced further but at the cost of fabrication tolerance. Given that the contact region is electrically isolated, the p-Ohmic contact (Ti/Pt/Au) is deposited directly onto the etched structure by PVD. An n-Ohmic global contact (AuGe/Ni/Au) is deposited on the back of the GaAs substrate by PVD in a similar manner to

the standard devices. The reduction in the number of processing steps means that VQF devices can be produced more than twice as quickly as the standard VCSELs.

For the qualification of the quick fabrication device performance, both device types are first processed on  $12.5 \times 12.5$  mm tile samples. Subsequently, the VQF process is applied to a full 4-inch (100 mm) wafer for spatial mapping and assessment of material uniformity. A diagram of the experimental setup is shown in Figure 2. Temperature-controlled on-wafer measurements are facilitated with a semi-automatic wafer mapper and a needle probe for electrical contact. Light is collected by an integrating sphere positioned such that the collection angle exceeds the beam divergence, hence capturing all the vertically emitted light. From this, an optical fibre tap is connected to a high-resolution spectrometer for the measurement of the lasing wavelength.

## 4 | RESULTS AND DISCUSSION

### 4.1 | Qualification of VQF at $\sim 895$ nm

The principal aim of VQF is to reduce the processing time (hence time-to-result), but the crucial benefit this brings about is timely characterisation of devices that are used to inform epitaxy. The performance, therefore, should be as representative as possible of a standard device structure. The methodology laid out in Ref. [8], for high-performance 940 nm VCSEL designs, is also used here to qualify VQF for  $\sim 895$  nm emitting devices. The VQF devices are found to approximate to the behaviour of BCB-planarised standard structures well across several aperture sizes.

The room temperature power-current characteristic, up to thermal rollover, for a VQF and standard device, with aperture sizes of 2 and 3  $\mu\text{m}$ , respectively, is shown in Figure 3. The standard VCSEL provides more optical power; however, this is to be expected given the larger aperture diameter. Slope efficiencies, calculated as the gradient of the light-current characteristic between 2 and 4 mA, are comparable, with a maximum value of approximately 0.3 W/A for both devices, occurring at 1.6–2 mA bias current. Thermal rollover occurs  $\sim 1$  mA lower bias current for the smaller aperture VQF device. Threshold currents are also comparable, 200  $\mu\text{A}$  for both devices, despite the difference in the aperture diameter. However, this is consistent with an increase in optical loss due to diffraction and scattering effects for small transverse dimensions [11, 12]. The series resistance of the standard VCSEL is found to be greater than that of the VQF device with resistance even with a larger active area. This effect was also seen previously in Ref. [8] and was associated with differences in contact resistances arising from the definition of the p-contact.

The comparable performance is unsurprising due to the large similarities in the epitaxial structure in this study compared with that of Ref. [8]. To avoid repetition, the full details of the extent of the experimental comparison that can be made are not included here. Instead, the focus of this study

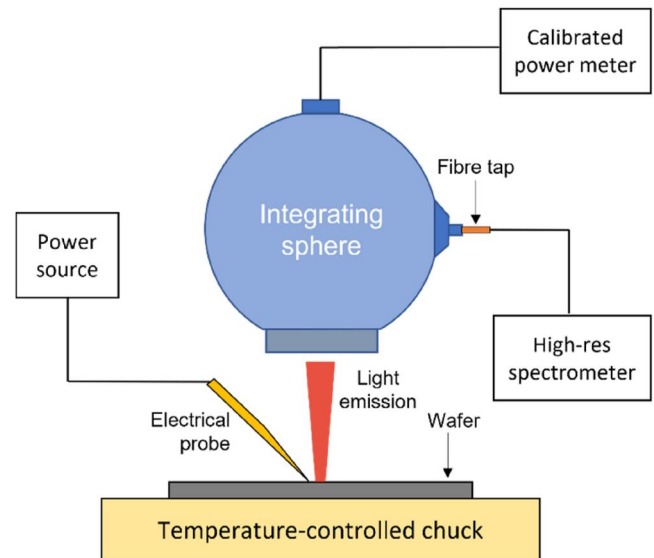


FIGURE 2 Setup for on-wafer characterisation of vertical cavity surface emitting laser (VCSEL) devices

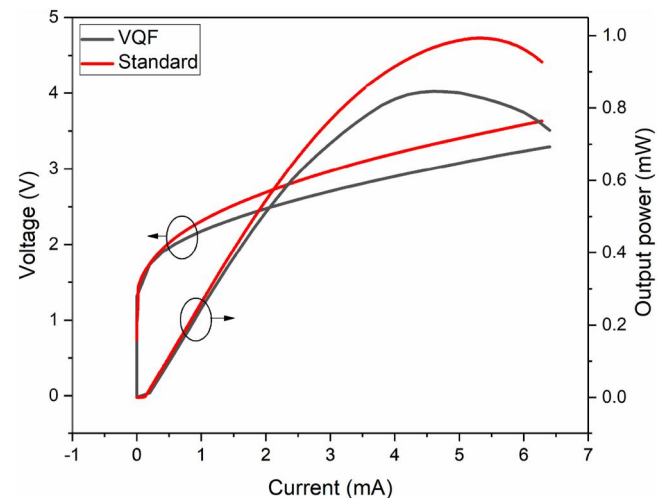


FIGURE 3 Power-current-voltage characteristic for a 2  $\mu\text{m}$  VCSEL quick fabrication (VQF) (black) and 3  $\mu\text{m}$  aperture standard (red)

is the application of VQF to assess material quality and uniformity in the context of high-volume production for MAC applications.

## 4.2 | Epi-material variation

### 4.2.1 | Oxidation

By characterising devices at many locations on a wafer, the spatial variation of the epi-layers is assessed. Additionally, the quality of the material itself can be ascertained, and the performance of VQF devices can be used to inform the design of the epi-structure. For this, the material variation must be disentangled from the variation due to fabrication, and one of the

most significant sources of this is the oxidation length non-uniformity. Figure 4 shows the as-grown wafer surface height/distortion variation of the AlGaAs-based VCSEL structure, which was grown on a 100 mm (4-inch) GaAs substrate for this study. The small lattice mismatch between the high-Al composition n-DBR layers and the GaAs substrate results in a significant bowing of the wafer [13]. This is approximately 100  $\mu\text{m}$  centre to edge for the 100 mm wafer.

This height variation can lead to a variation in wafer temperature during wet thermal oxidation, and owing to the exponential dependence on temperature, results in a significant variation in the oxidation length across the wafer. Figure 5 shows  $\sim 2 \mu\text{m}$  variation of the in-situ measured oxidation lengths. The non-uniform spatial dependence is a cumulative result of the radial variation in the wafer temperature associated with the bowing and a resulting non-uniformity in the furnace temperature. Better oxidation uniformity can be obtained with the help of extra steps in fabrication to reduce wafer bow (substrate-side deposition of a strain reducing layer) or through alternative oxidation methods. The effectiveness and trade-offs in these approaches will be discussed below.

#### 4.2.2 | Lasing wavelength

For MAC applications, control of the laser emission wavelength is critical and substantially more stringent than the conventional VCSEL applications, such as datacoms, and is one of the key challenges with large-scale MOCVD growth with the target specification within  $\pm 2 \text{ nm}$  of the target wavelength. The existing wafer characterisation techniques involve the measurement of the material cavity mode wavelength, which is extracted from the reflectivity spectrum. This is routinely measured at many locations post-growth, and the resulting contour plot for this wafer is shown in Figure 6. The variation is generally radial

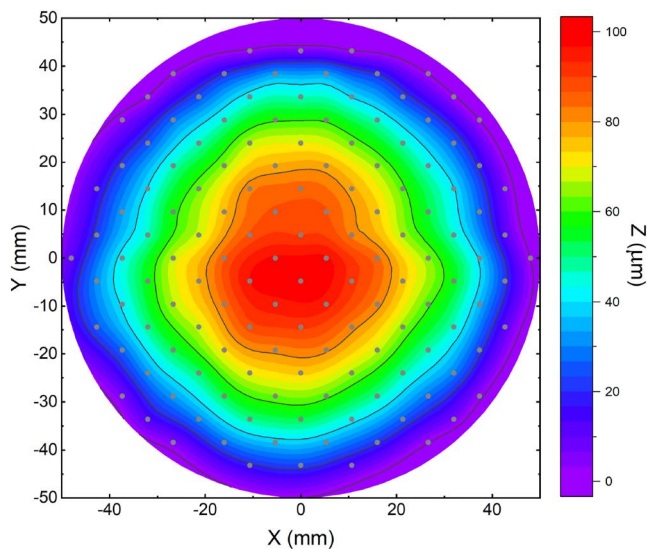


**FIGURE 4** Height variation of a 4-inch wafer, showing the strain-induced wafer bow resulting from the growth on a GaAs substrate

with a decrease in the resonance wavelength towards the edge, which is associated with a decrease in the optical path length of the inner cavity and controlled by the thickness and composition during the epi growth. The room temperature lasing wavelength at 2 mA injection current for large apertures ( $\sim 8 \mu\text{m}$  at the wafer centre) across the same wafer is shown in Figure 7, and there is a good agreement with the spatial dependence of the cavity mode wavelength. The lasing wavelengths are blue-shifted relative to the target specification; however, it should be noted that the room temperature target wavelength is below 894.6 nm to facilitate high-temperature operations. For MACs, large-aperture VCSELs are undesirable given their multi-mode emission. However, one of the benefits of looking at the wavelength variation for these larger devices is that scattering/diffraction effects of small-aperture devices can be excluded, and the impact of oxide aperture non-uniformity is less significant, which

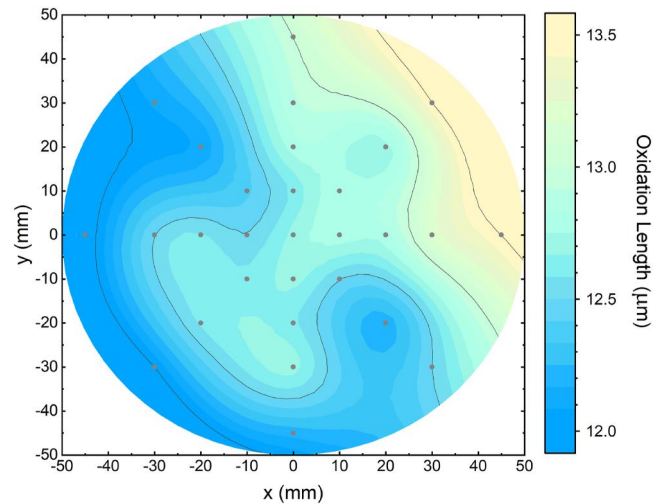


**FIGURE 5** Spatial variation of the in-situ measured oxidation length, resulting from temperature non-uniformities

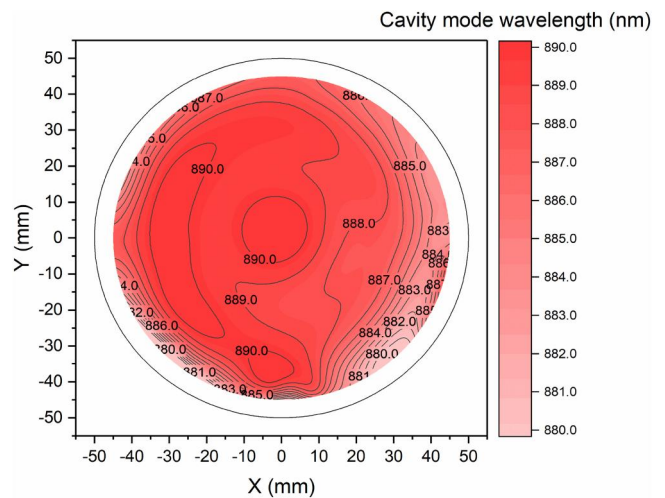


**FIGURE 6** Spatial variation of the material cavity mode wavelength extracted from reflectivity measurements at 25°C

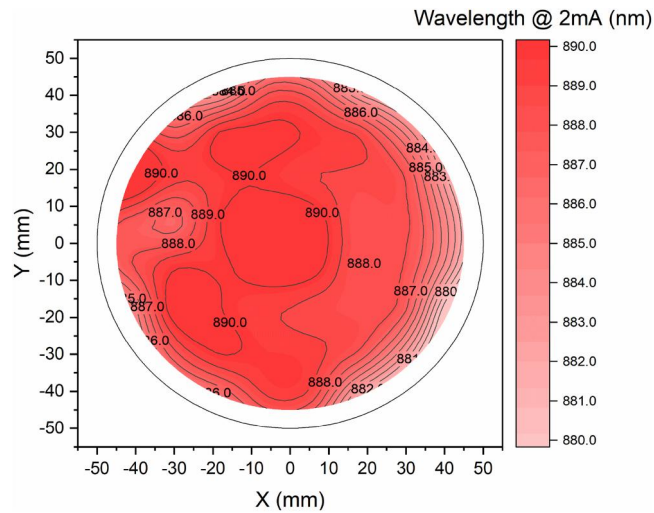


**FIGURE 7** Variation of fundamental mode wavelength at 25°C for 36  $\mu\text{m}$  mesa VCSEL quick fabrication (VQF) devices ( $\sim 8 \mu\text{m}$  aperture at the centre)

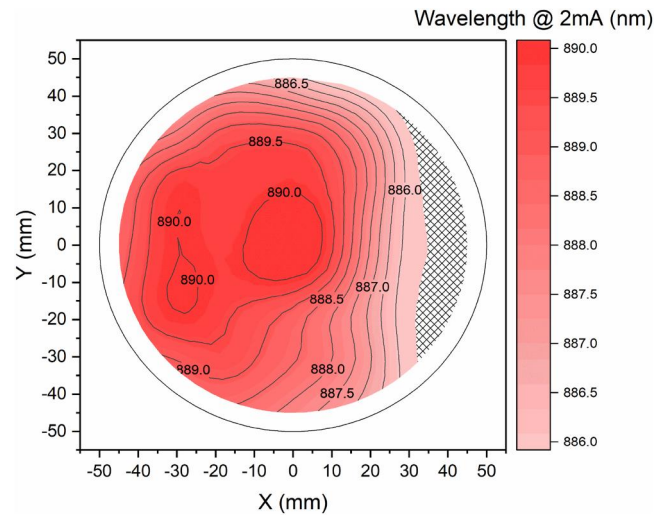


**FIGURE 8** Variation of fundamental mode wavelength at 25°C of 32  $\mu\text{m}$  mesa VCSEL quick fabrication (VQF) devices ( $\sim 4 \mu\text{m}$  aperture at the centre)

disentangles the effects of device heating from the measurement. Therefore, the effect of the epi-layer variation can be isolated.

Conversely, it is also useful to consider the yield of devices, which best mimic the desired application. In Figure 8, the room temperature lasing wavelength at 2 mA is mapped for small aperture devices ( $\sim 4 \mu\text{m}$  at the centre). For the working devices, the wavelengths match well with the larger aperture devices with some redshift due to higher current densities. Further, the effect of oxide aperture non-uniformity can be seen clearly by the data missing on the east of the wafer. For these mesa sizes, the VCSEL apertures are fully closed owing to the variation in the oxidation length. Despite this, the working devices are more representative of that, which would be used in a MAC package where a single-mode emission is required. This is extended in Figure 9 where the wavelengths for these same devices are mapped at 70°C.

There is a large area towards the centre of the wafer where the VQF device fundamental mode emits at 894.6 nm for approximately 4  $\mu\text{m}$  aperture devices; however, this occurs at 6 mA, which is higher than the intended operating current. Nevertheless, this provides valuable information to inform design and growth iterations. Given that it is the fundamental mode emitting at 894.6 nm, standard surface-relief techniques can be applied to suppress high-order modes and achieve the single-mode emission. The insight gained here is the variation of operating conditions and device geometries to meet the target specifications, which is the advantage of VQF, as well as enabling the analysis of performance at high and low temperatures, thus providing a better understanding of what room temperature performance will result in a desired performance at the intended operating conditions.

#### 4.2.3 | Laser threshold

The VCSEL threshold current is another important consideration in the device specification for MACs. In Figure 10, a

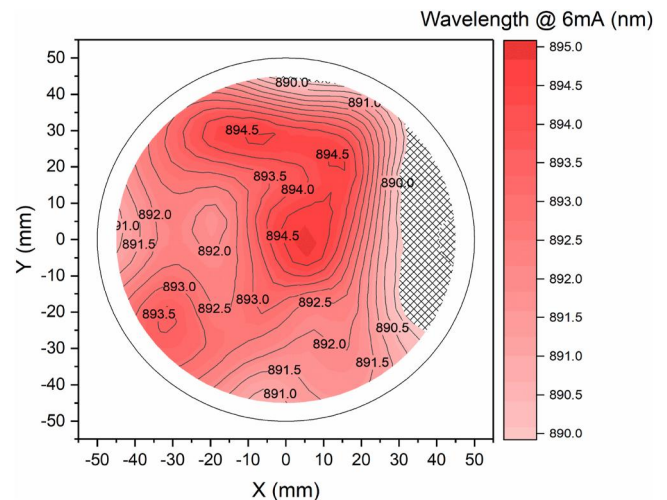


**FIGURE 9** Variation of fundamental mode wavelength of 32  $\mu\text{m}$  mesa VCSEL quick fabrication (VQF) devices ( $\sim 4 \mu\text{m}$  aperture at the centre) at 70°C

contour plot of the VQF device threshold current is shown and the spatial dependence is found to track with the oxidation length variation, as shown in Figure 6, which is expected given that the laser threshold current is proportional to the active volume. Therefore, to remove the influence of fabrication variations on the assessment of material quality and uniformity, the variation in threshold current density should be considered.

This point is illustrated by the plots of Figure 11, which show the variation in the threshold current density with mesa diameter (left) and oxide aperture diameter (right). When looking at values for equivalent mesa diameters at different regions of the wafer, the effect of the oxidation non-uniformity is neglected. However, when the difference in the oxidation length, hence oxide aperture, is considered, the comparison of

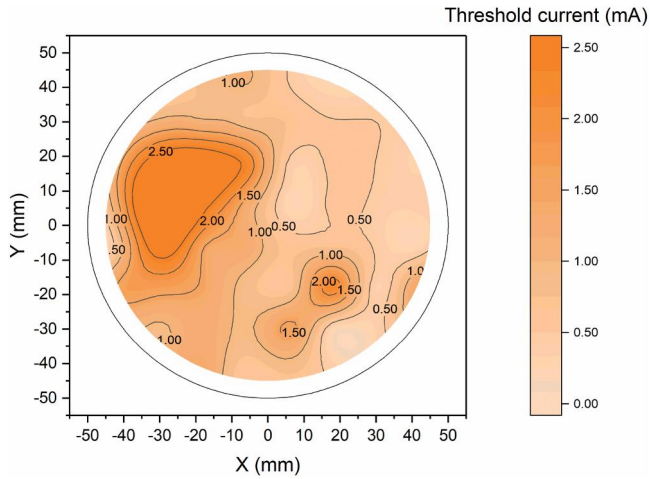


**FIGURE 10** Variation of threshold current of  $36\ \mu\text{m}$  mesa VCSEL quick fabrication (VQF) devices ( $\sim 8\ \mu\text{m}$  aperture at the centre)

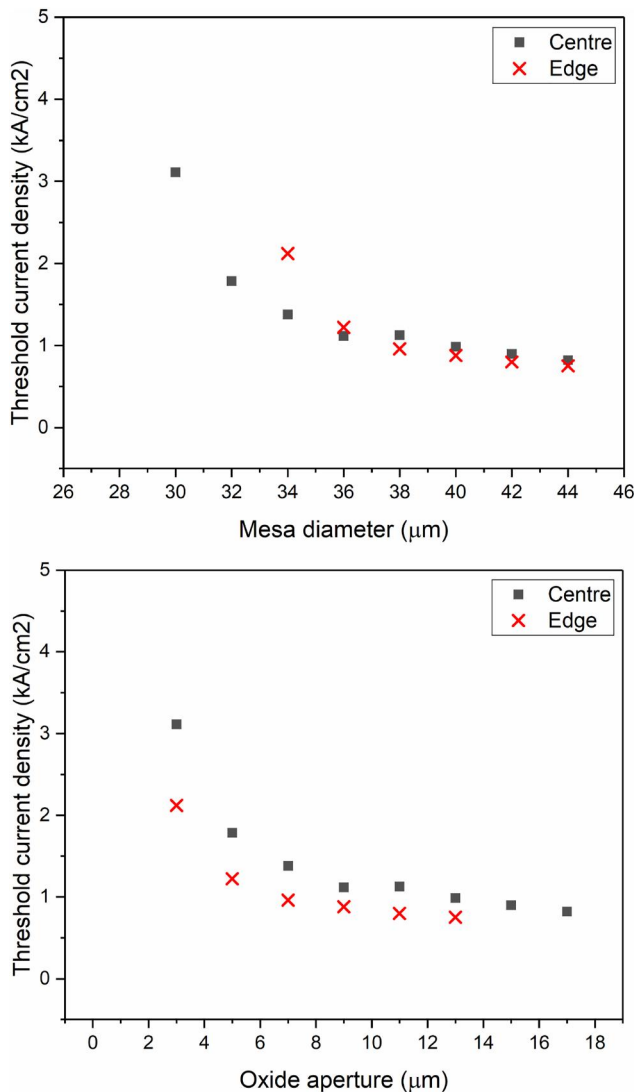


**FIGURE 11** Variation of threshold current density with mesa diameter (top) and oxide aperture diameter (bottom) for edge (red cross) and centre (black square) materials

equal aperture devices yields a very different result. This further demonstrates why mapping performance of larger devices provides more reliable information on material variations. It is found that, for equivalent aperture diameters, the VQF threshold current density is lower at the wafer edge than at the centre—hence it is driven by a variation in the epitaxy—associated with a reduced optical loss.

#### 4.2.4 | Device efficiency and output power

Similarly, the slope efficiency of the final VCSEL is of interest, and the spatial variation is mapped across the wafer. For MAC applications, it is not necessary to maximise the slope efficiency, but to limit it instead. A high slope efficiency can lead to output power instability, which is not desirable for CPT optical pumping. Hence a maximum of  $0.5\ \text{W/A}$  is targeted. The variation in slope efficiency across the wafer is shown in Figure 12. It can be seen that the regions of the lower slope efficiency coincide with the regions of the high threshold current (see Figure 10), which is attributed to these areas having a shorter oxidation length.

The same can be seen for the variation in output power in Figure 13. Given that the power is measured at  $3\ \text{mA}$  bias current, the higher threshold current (larger aperture) devices are again closer to the threshold; hence, the power delivered is lower than that of the smaller aperture devices.

With respect to the target specification, the output power of the VCSEL at the operating current ( $3\ \text{mA}$ ) is designed to be maximised and deliver at least  $0.6\ \text{mW}$ . However, the output powers measured here, which exceed the target, are not directly representative of a full structure. The multi-mode VQF emission has a higher output power than the intended single-mode emission—the same can be said for VQF slope efficiencies. Hence, with the comparison of these results to that of single-mode operating devices, this relationship is understood and VQF can therefore infer an expected performance.

#### 4.2.5 | Gain-peak detuning

Another important consideration for optimising device performance is the detuning of the gain peak wavelength and resonant cavity-mode wavelength. When the two coincide, the electrical pumping required (carrier density) for lasing is minimised; however, owing to the large difference in the shift of these wavelengths with temperature, it is advantageous to have a detuning at room temperature. The spectral peak of the gain shifts at  $\sim 0.3\ \text{nm/K}$ , associated with bandgap narrowing, compared to  $\sim 0.06\text{--}0.07\ \text{nm/K}$  associated with refractive index shift for the cavity mode; hence, a detuning of the cavity mode to the long wavelength side of the gain spectrum means that the alignment occurs above the room temperature [14]. With target operation  $\geq 70^\circ\text{C}$ , the detuning should be sufficient to facilitate the alignment at these temperatures. On the other hand, the linewidth of the VCSEL spectra also needs to be considered, and the

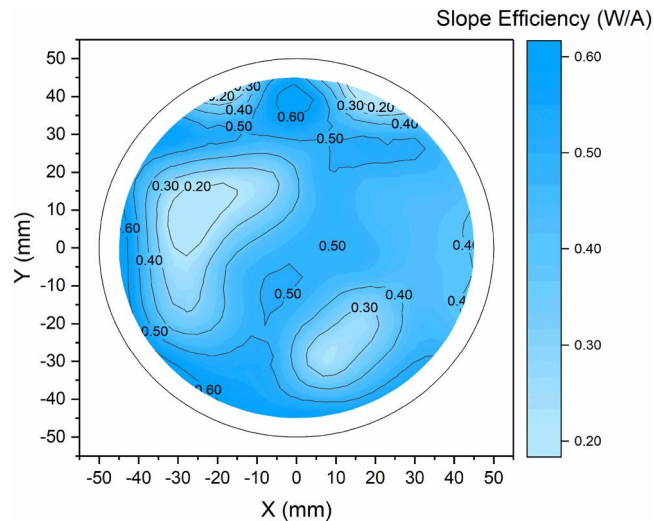


**FIGURE 12** Variation of slope efficiency of 36  $\mu\text{m}$  mesa VCSEL quick fabrication (VQF) devices ( $\sim 8 \mu\text{m}$  aperture at the centre)

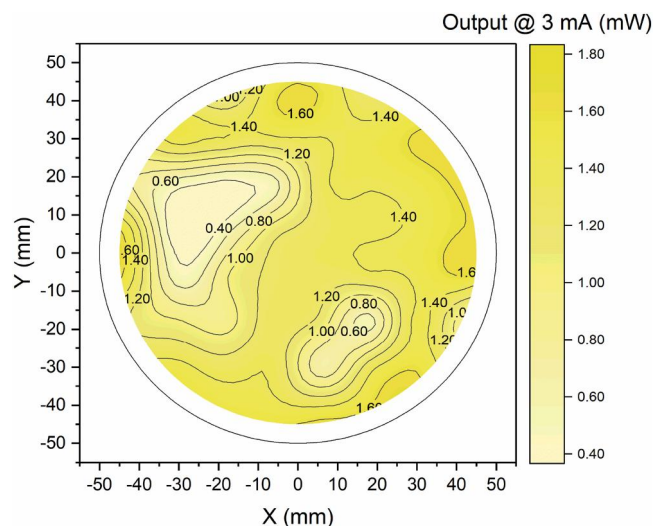


**FIGURE 13** Variation of output power at 3 mA of 36  $\mu\text{m}$  mesa VCSEL quick fabrication (VQF) devices ( $\sim 8 \mu\text{m}$  aperture at the centre)

operation on the short wavelength side of the gain spectrum can work to reduce linewidth and the linewidth enhancement factor [15, 16].

By measuring the threshold current density as a function of temperature, the temperature at which the gain peak and cavity mode align can be ascertained. This is shown in Figure 14 for large mesa VQF devices from the centre and edge of the wafer. The centre device has a minimum at  $\sim 50^\circ\text{C}$  compared to the minimum for the edge device that occurs close to the room temperature. Therefore, the device at the edge is found to operate at zero detuning at room temperature; any subsequent increase in the operating temperature shifts the cavity mode away from alignment with the gain peak and requires higher pumping for lasing and hence a higher threshold current density. Conversely, the threshold requirement for the centre device decreases with the increasing temperature, and at  $70^\circ\text{C}$ , the

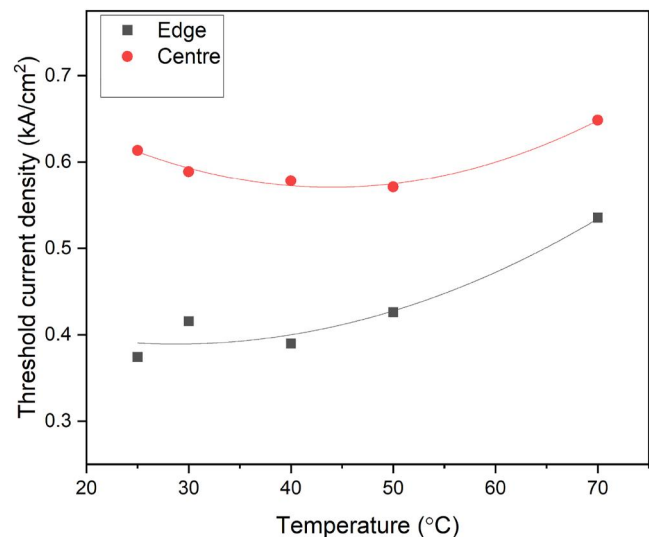


**FIGURE 14** Temperature dependence of threshold current density for 36  $\mu\text{m}$  mesa VCSEL quick fabrication (VQF) devices at the centre and edge of a 4-inch wafer

devices from both locations operate on the short wavelength side of the gain spectrum and with a similar threshold current density. Therefore, the detuning works to improve the device yield at  $70^\circ\text{C}$  by improving the uniformity in the threshold, a characteristic that cannot be determined through conventional assessment of epi-structures during the manufacturing process. Additionally, based on the temperature alignment, the room temperature detuning is calculated as 1.5 nm with the room temperature gain peak wavelength approximately at 884.8 nm. These values can be directly compared to the modelling results from the design of the structure and post-growth wafer characterisation (PL) to assess the quality of epitaxy. It is also found that, due to this detuning, the devices at both the centre and edge of wafer operate on the short wavelength side of the gain spectrum, which is important in predicting limits to the device linewidth across the wafer.

## 5 | CONCLUSION

VCSEL quick fabrication has been applied to the epi-material, which is designed for an 894.6 nm emission wavelength for miniature atomic clock applications. The characterisation of VQF devices is used to assess material quality and uniformity against target specifications in terms of lasing wavelength, threshold behaviour, device efficiency, and output power. A significant fraction of the wafer produces devices, which operate at the target wavelength of 894.6 nm at  $70^\circ\text{C}$ ; however, this occurs at an injection current higher than the intended operation levels. The oxide aperture variation is shown to further limit the device yield. In terms of the threshold current (density), differential efficiency, and optical power, the on-wafer yield is high and principally limited by the oxide aperture non-uniformity. The threshold current density is observed to vary across the wafer from centre to edge, implying a difference

in the gain peak-to-cavity resonance detuning; however, the VQF data reveals that this variation reduces closer to the intended operating temperature; a noteworthy assessment of uniformity that is not accessible using standard epi characterisation during the manufacture process. While there are some inherent differences in terms of optical power and efficiency between VQF devices and conventional single-mode devices required for MACs, the information gained about the on-wafer variation is valuable, and the data can inform whether the stringent performance targets will be met. The same measurement is used to extract the room temperature gain peak wavelength at different locations on the wafer, which can be directly compared to modelling and post-growth measurements to assess the quality of growth.

### AUTHOR CONTRIBUTIONS

**Sara Gillgrass:** Investigation; Methodology. **Tomas Peach:** Investigation; Methodology. **James Meiklejohn:** Data curation. **Curtis Hentschel:** Data curation; Investigation. **Tracy Sweet:** Conceptualization; Resources. **Denise Powell:** Investigation; Resources. **Wyn Meredith:** Resources. **J. Iwan Davies:** Conceptualization; Resources; Supervision. **Samuel Shutts:** Conceptualization; Funding acquisition; Project administration; Supervision. **Peter M. Smowton:** Funding acquisition; Project administration; Supervision.

### ACKNOWLEDGEMENTS

This work was supported in part by the Engineering and Physical Sciences Research Council (EPSRC) Future Compound Semiconductor Manufacturing Hub, under Grant EP/P006973/1, in part by the European Regional Development Fund through SMART Expertise Project, ATLAS under Grant 82371, and in part by the Strength in Places Fund under Project 107134. J. Baker and C. Hentschel acknowledge support from an EPSRC-funded iCASE PhD studentship supported by IQE plc. under Grants EP/T517525/1 and EP/S513611/1.

### CONFLICT OF INTEREST

The authors declare no conflicts of interest.

### DATA AVAILABILITY STATEMENT

Due to confidentiality agreements with research collaborators, supporting data can only be made available to bona fide researchers subject to a non-disclosure agreement. Details of the data and how to request access are available at the Cardiff University Research Data Archive at <http://doi.org/10.17035/d.2002.0230257036>.

### ORCID

Jack Baker  <https://orcid.org/0000-0003-1379-0673>

### REFERENCES

1. Kitching, J., et al.: A microwave frequency reference based on VCSEL-driven dark line resonances in Cs vapor. *IEEE Trans. Instrum. Meas.* 49(6), 1313–1317 (2000). <https://doi.org/10.1109/19.893276>
2. Serkland, D.K., et al.: VCSELs for Atomic Sensors, vol. 6484, pp. 48–57. Feb (2007). <https://doi.org/10.1117/12.715077>
3. Vanier, J., Godone, A., Levi, F.: Coherent population trapping in cesium: dark lines and coherent microwave emission. *Phys. Rev.* 58(3), 2345–2358 (1998). <https://doi.org/10.1103/PhysRevA.58.2345>
4. Affolderbach, C., et al.: Nonlinear spectroscopy with a vertical-cavity surface-emitting laser (VCSEL). *Appl. Phys. B* 70(3), 407–413 (2000). <https://doi.org/10.1007/S003400050066>
5. Miah, M.J., et al.: Fabrication and characterization of low-threshold polarization-stable VCSELs for Cs-based miniaturized atomic clocks. *IEEE J. Sel. Top. Quant. Electron.* 19(4), 1701410 (2013). <https://doi.org/10.1109/JSTQE.2013.2247697>
6. Gruet, F., et al.: Metrological characterization of custom-designed 894.6 nm VCSELs for miniature atomic clocks. *Opt Express* 21(5), 5781–5792 (2013). <https://doi.org/10.1364/OE.21.005781>
7. Zaouris, D., et al.: MacV: VCSELs for miniature atomic clocks. In: IFCS/EFTF 2019 - Jt. Conf. IEEE Int. Freq. Control Symp. Eur. Freq. Time Forum, Proc (2019). <https://doi.org/10.1109/FCS.2019.8856005>
8. Baker, J., et al.: VCSEL quick fabrication for assessment of large diameter epitaxial wafers. *IEEE Photon. J.* 14(3), 1–10 (2022). <https://doi.org/10.1109/JPHOT.2022.3169032>
9. Baker, J., et al.: Sub-mA threshold current vertical cavity surface emitting lasers with a simple fabrication process. In: 2021 IEEE Photonics Conf, pp. 1–2 (2021). <https://doi.org/10.1109/IPC48725.2021.9592977>
10. Martinsson, H., et al.: Transverse Mode Selection in Large Area Oxide-Confined VCSELs Using Shallow Surface Reliefs, pp. 49–50. LEOS Summer Top. Meet. (1999). <https://doi.org/10.1109/leosst.1999.794709>
11. Hegblom, E.R., et al.: Scattering losses from dielectric apertures in vertical-cavity lasers. *IEEE J. Sel. Top. Quant. Electron.* 3(2), 379–389 (1997). <https://doi.org/10.1109/2944.605682>
12. Thibeault, B., et al.: Electrical and optical losses in dielectrically apertured vertical-cavity lasers. In: Vertical-Cavity Surface-Emitting Lasers, vol. 3003, pp. 86–99 (1997). <https://doi.org/10.1117/12.271055>
13. Baker, J., et al.: Impact of strain-induced bow on the performance of VCSELs on 150mm GaAs- and Ge-substrate wafers. *Semicond. Lasers Laser Dynam. X* PC12141, PC1214108 (2022). <https://doi.org/10.1117/12.2624492>
14. Wu, J., Xiao, W., Lu, Y.M.: Temperature and wavelength dependence of gain and threshold current detuning with cavity resonance in vertical-cavity surface-emitting lasers. *IET Optoelectron.* 1(5), 206–210 (2007). <https://doi.org/10.1049/iet-opt:20070039>
15. Kuskonov, D., et al.: Linewidth and  $\alpha$ -factor in AlGaAs/GaAs vertical cavity surface emitting lasers. *Appl. Phys. Lett.* 66(3), 277–279 (1995). <https://doi.org/10.1063/1.113516>
16. Yu, S.F.: Analysis and Design of Vertical Cavity Surface Emitting Lasers. John Wiley & Sons, Inc. (2005)

**How to cite this article:** Baker, J., et al.: VCSEL quick fabrication of 894.6 nm wavelength epi-material for miniature atomic clock applications. *IET Optoelectron.* 1–8 (2022). <https://doi.org/10.1049/ote2.12082>